

# Ab-initio investigation of electronic and optical properties of $\text{InAs}_{1-x}\text{P}_x$ alloys

Mazin OTHMAN<sup>1\*</sup>, Ergun KASAP<sup>1</sup>, Nurettin KOROZLU<sup>1</sup>

<sup>1</sup>Gazi University, Faculty of Art and Science, Department of Physics, Ankara, Turkey

Received: 24.07.2009 Revised: 24.12.2009 Accepted: 05.01.2010

---

## ABSTRACT

The electronic energy band structure and linear optical properties  $\text{InAs}_{1-x}\text{P}_x$  alloys are investigated by an ab initio pseudopotential method using density functional theory in the local density approximation (LDA) and a scissors approximation. The calculated band gap energy and density of state (DOS). Electronic band structure shows that  $\text{InAs}_{1-x}\text{P}_x$  alloys are direct band gap and the optical band gap increase from 0.24 to 1.20 eV with increasing P concentrations. The linear energy dependent dielectric functions and some optical properties such as absorption, energy loss function refractive index and reflectivity calculated. Our results agree well with the available data in the literature.

**Key Words:** Alloys, Electronic structures, Optical properties.

---

## 1. INTRODUCTION

Semiconductor alloys are made of elements from group III and group V on the periodic table such as InAs that is commonly used to interact with light in typical optical devices. InAsP ternary phosphates are potentially useful for optoelectronic device applications. InAsP is a wide band-gap alloy that is often employed in red light emitting diodes (LEDs) [1, 2]. InAsP is a useful material for long-wavelength surface emitting lasers [3]. Although some experimental and theoretical investigations have been reported on the band-structure parameters for III-V crystalline phases with zinc-blend structure [4, 5] many fundamental properties of these materials remain to be determined precisely. Today, the production and the use of InAs with technological devices with added P become more important gradually, increase more and more. Experimental studies on such type of produced semiconductor alloys are carried out intensively. This study was carried out to shed light on the future studies of scientists who experimentally prepare and test these alloys in laboratories to help them in determining the change in amounts of additives in alloys, and to determine the accordance of theoretical studies with experiments and other theoretical works. In the end, features of new semiconductor alloys that may

be obtained by adding P to InAs structure at various ratios were examined.

In this study, electronic and optical properties of  $\text{InAs}_{1-x}\text{P}_x$  alloys (for  $x= 0, 0.25, 0.50, 0.75$  and 1) were calculated as a function of P composition by using Cambridge Serial Total Energy Package (CASTEP) program [6] that is based on the density functional theory (DFT) by Kohn and Sham [7]. Obtained results were found in good agreement compared with experimental and theoretical data in literature. The layout of this paper is given as followings: The method of calculation is given in Section 2. The results and overall conclusion are presented and discussed in Section 3 and 4, respectively.

## 2. METHOD OF CALCULATION

The electronic wavefunctions were obtained by using a density-mixing minimization method for the self-consistent field (SCF) calculation, and the structures were relaxed by using the Broyden, Fletcher, Goldfarb and Shannon (BFGS) method [8]. It solves the quantum mechanical equation for the electrons within the density functional approach in the local-density approximation (LDA). For LDA, the exchange-correlation functional of Ceperley and Adler [9], as parameterized by Perdew

---

\*Corresponding author, e-mail: mazin@gazi.edu.tr

and Zunger [10], is used. The orbital's of As ( $4s^2 4p^3$ ), In ( $4d^{10}5s^2 5p^1$ ), and P ( $3s^2 3p^3$ ) are treated as valence electrons.

The tolerances for geometry optimization were set as the difference in total energy being within  $5 \times 10^{-6}$  eV/atom, the maximum ionic Hellmann-Feynman force within  $0.01$  eV/Å, the maximum ionic displacement within  $5 \times 10^{-4}$  Å, and the maximum stress within  $0.02$  GPa. The interactions between electrons and core ions are simulated with separable Troullier–Martins [11] norm-conserving pseudopotentials. A cubic unit cell is constructed with four group III atoms (As/P) and four group V atoms (P). We have considered  $\text{InAs}_{1-x}\text{P}_x$  ternary alloys as having cubic symmetry in our calculation for all the five systems to maintain consistency and simplicity. We expect that for  $x = 0.5$  the alloy is a layered structure and should be non-cubic. We have taken four layers and hence a cubic unit cell for  $x = 0.25, 0.50, 0.75$  we have replaced one, two and three As atoms, respectively, by In to get the desired concentration. The idea of constructing an alloys by taking a large unit cell (cubic eight-atom) and repeating it three dimensionally for the calculation of the electronic structure of the semiconductor alloy has been used by Agrawal et al [17] have used an eight-atom cubic super cell to calculate the electronic properties of  $\text{In}_x\text{Ga}_{1-x}\text{P}$  alloys, although no such calculations have been performed for  $\text{In}_x\text{Ga}_{1-x}\text{P}$  ternary alloys The wave functions are expanded in the plane waves up to a kinetic- energy cutoff of  $880$  eV. In this work, the k-points of  $6 \times 6 \times 4$  for  $x=0.5$  and  $4 \times 4 \times 4$  for the other composition  $x$ , which are in the Monkhorst and Pack scheme, are used.

### 3. RESULTS AND DISCUSSION

#### 3.1. Electronic Properties

The band structures of the alloys show similar features to that of bulk InAs and InP. However, even accounting for the folded bands in the larger unit cell alloy systems, there are important points to note. At the top of the valence band at  $\Gamma$ , the degeneracy is broken even in the absence of spin-orbit or strain effects. It is directly due to the presence of unequal bond lengths in the unit cell. Also, at symmetry points the electron energies in the alloys are not simple averages of those findings in InAs and InP.

We have predicted the band structure for  $\text{InAs}_{1-x}\text{P}_x$  along the high symmetry directions in the first Brillouin zone and corresponding density of states from the calculated equilibrium lattice constant. For all compositions ( $x$ ), the calculated band structures and DOS are compatible with each other. The bands and DOS graphs are given in Figure 1 only for  $x = 0.25$  to save space in journal. All these mixed crystals have a direct band gap along the  $\Gamma$  direction, and the obtained results are listed in Table 1 along with the other theoretical and experimental data [5, 12-14]. The band profiles and band gap values are in good agreement with the earlier theoretical works. The band gaps are smaller than the experimental values because of the use of the LDA in our calculations. The energies of band- gaps versus

composition  $x$  (0, 0.25, 0.5, 0.75, and 1) for  $\text{InAs}_{1-x}\text{P}_x$  are shown in Figure 2 Here the composition dependence of band gap energy exhibits almost a linear decreasing trend.

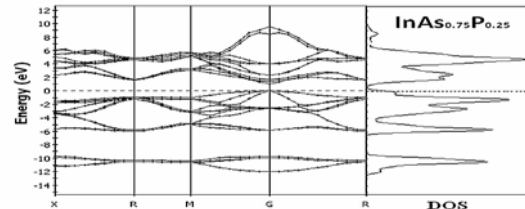


Figure 1. Calculated band structure and DOS of  $\text{InAs}_{0.75}\text{P}_{0.25}$

Table 1. Band gap energies of  $\text{InAs}_{1-x}\text{P}_x$

Material	reference	Energy Bandgap (eV)
InAs	Present	0.24
	Theory <sup>a</sup>	0.30
	Theory <sup>b</sup>	0.19
	Expt. <sup>c</sup>	0.35
In $\text{As}_{0.75}\text{P}_{0.25}$	Present	0.68
	Expt. <sup>d</sup>	0.77
In $\text{As}_{0.5}\text{P}_{0.5}$	Present	0.98
	Expt. <sup>d</sup>	1.24
In $\text{As}_{0.25}\text{P}_{0.75}$	Present	1.12
	Expt. <sup>d</sup>	1.30
InP	Present	1.20
	Theory <sup>a</sup>	1.23
	Theory <sup>b</sup>	1.34
	Expt. <sup>c</sup>	1.39

<sup>a</sup>Ref. [12], <sup>b</sup>Ref. [5], <sup>c</sup>Ref. [13], <sup>d</sup>Ref. [14]

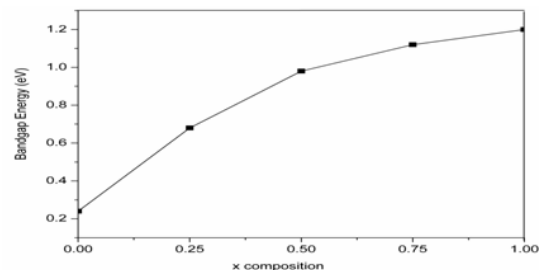


Figure 2. Band gap energies of  $\text{InAs}_{1-x}\text{P}_x$

#### 3.2. Optical Properties

To investigate the optical band gap and optical transition of  $\text{InAs}_{1-x}\text{P}_x$  system, it is necessary to investigate the imaginary part of the dielectric function ( $\epsilon_2$ ) because ( $\epsilon_2$ ) is very important for optical properties of every material. It is well known that the interaction of a photon with the electrons in the system

can be described in terms of time dependent perturbations of the ground-state electronic states. Optical transitions between occupied and unoccupied states are caused by the electric field of the photon. The spectra from the excited states can be described as a joint DOS between the valence and conduction bands. The momentum matrix elements, which are used to calculate the  $(\epsilon_2)$ , are calculated between occupied and unoccupied states, which are given by the eigenvectors obtained as the solution of the corresponding Schrödinger equation. Evaluating these matrix elements, one uses the corresponding eigenfunctions of each of the occupied and unoccupied states. The real part of the dielectric function  $(\epsilon_1)$  can be evaluated from the imaginary part  $(\epsilon_2)$  by the famous Kramers–Kronig relationship. Absorption coefficient  $\alpha(\omega)$  can be obtained from  $(\epsilon_1)$  and  $(\epsilon_2)$

$$\alpha(\omega) = \sqrt{2} \omega \left[ \sqrt{\epsilon_1^2(\omega) + j\epsilon_2^2(\omega)} - \epsilon_1(\omega) \right]^{1/2} \dots(1)$$

Figure 3 gives the imaginary part of the dielectric function of  $\text{InAs}_{1-x}\text{P}_x$  alloys. The prominent peaks which are mainly related to the interband transition occur at about 4.8, 4.7, 4.5, 4.3 and 4.6 eV, respectively. Figure 4 gives the optical absorption spectra of the  $\text{InAs}_{1-x}\text{P}_x$  system under the scissor operation in the range of 0–2 eV. Due to the underestimation of the band gap, it is difficult to obtain the exact optical band gap. In our calculations, we have used the energy scissor approximation with 0.6 eV to fit the absorption edge to the experimental value. This method is effective for a variety of systems [15]. It is well known that the relation between the optical band gap and the absorption coefficient is given by [16]

$$\alpha h\nu = c (h\nu - E_g)^{1/2} \dots\dots\dots(2)$$

where  $h$  is the Planck constant,  $c$  is a constant for a direct transition,  $\nu$  is the frequency of radiation, and  $\alpha$  is the optical absorption coefficient. The optical band gap  $E_g$  can be obtained from the intercept of  $(\alpha h\nu)^2$  versus photon energy  $(h\nu)$ . By using the extrapolation, the optical band gap of  $\text{InAs}_{1-x}\text{P}_x$  can be obtained.

The optical band gap depending on P concentration has been shown in the inset. It can be observed that the optical band gap increases from 0.24 to 1.42 eV with increasing P concentrations, which is in good agreement with the previous experimental investigations [14].

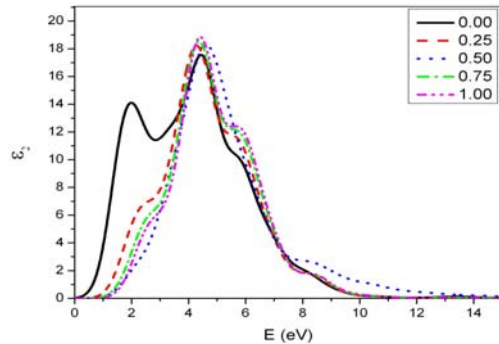


Figure 3. The imaginary part of the dielectric function of  $\text{InAs}_x\text{P}_{1-x}$  alloys.

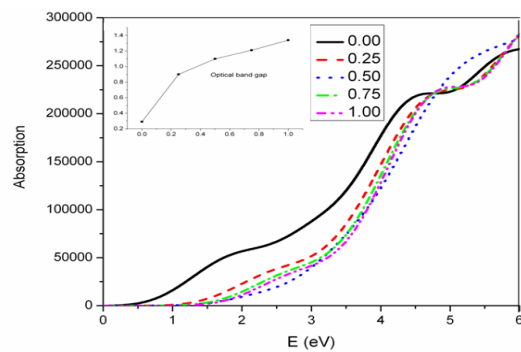
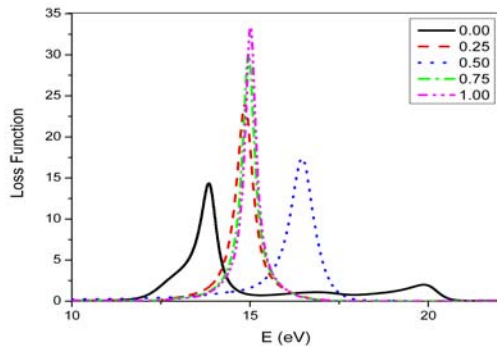
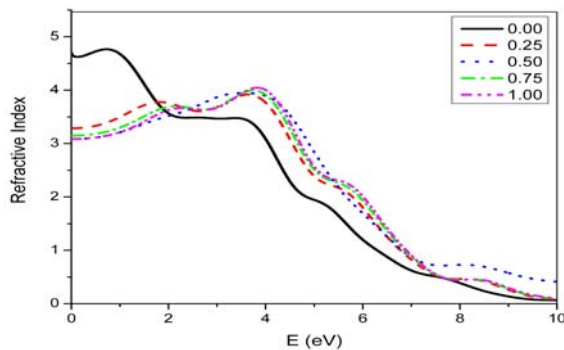
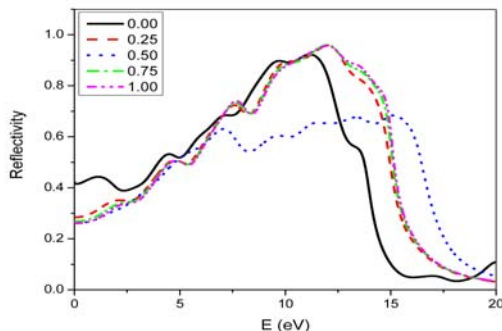


Figure 4. Optical absorption of  $\text{InAs}_{1-x}\text{P}_x$  alloys.

Figure 5, 6 and 7 give the optical constants of  $\text{InAs}_{1-x}\text{P}_x$  alloys in the range of 0–20 eV. The optical constants, such as loss function, reflectivity and refractive index, are very important for the optical materials and related applications. Overall, the optical constants of the  $\text{InAs}_{1-x}\text{P}_x$  alloys have slightly changed. For example, the loss function spectra Figure 5, describes the energy loss of a fast electron traversing in  $\text{InAs}_{1-x}\text{P}_x$  alloys. The peaks of 13.9, 14.7, 16.3, 15.1 and 15 respectively in the loss function are plasma resonance peaks and they are also the points of transition from the metallic property to the dielectric properties for  $\text{InAs}_{1-x}\text{P}_x$ .

The knowledge of the refractive index of the  $\text{InAs}_{1-x}\text{P}_x$  alloys is necessary for accurate modelling and design of devices. The refractive index and reflectivity of  $\text{InAs}_{1-x}\text{P}_x$  increase in the low energy range, which indicate that the band gap increases [14]. The dispersion curves of refractive indices are plotted in figure 5 for each composition  $x$ , and the refractive indices  $n(0)$  for  $\text{InAs}_{1-x}\text{P}_x$  are found to be 4.5, 3.3, 3.1, 3.2 and 3.0, respectively.

Figure 5. Loss function of InAs<sub>1-x</sub>P<sub>x</sub> alloysFigure 6. Refractive Index of InAs<sub>1-x</sub>P<sub>x</sub> alloys.Figure 7. Optical reflectivity of InAs<sub>1-x</sub>P<sub>x</sub> alloys.

#### 4. CONCLUSIONS

In summary, we have presented electronic and optical properties of the InAs<sub>1-x</sub>P<sub>x</sub> alloys, using the first principles methods. Specifically, energy band gap have been calculated and consistent results are obtained. For all compositions these alloys are characterized by direct band gap materials along the  $\Gamma$  direction. The optical properties of the InAs<sub>1-x</sub>P<sub>x</sub> alloys have been presented in details. The investigation shows that as P composition increases in the alloys, band gap energy increase whereas and refractive index decrease. These results are also consistent with the Vegard's law. It is hoped that the present findings may provide reliable data for producing optoelectronic devices.

#### ACKNOWLEDGEMENTS

The authors would like to thank Assistant Researcher Murad Sherzad Othman for some helpful suggestions

and discussions. This work is supported by Gazi University Research-Project Unit under Project No: 05/2008/42.

#### REFERENCES

- [1] Smokal, V., Derkowska, B., Czaplicki, R., "Nonlinear optical properties of Zn<sub>1-x</sub>Mg<sub>x</sub>Se and Cd<sub>1-x</sub>Mg<sub>x</sub>Se crystals", *Optical Materials*, 31: 518–522 (2009).
- [2] Chen, A-B., Sher, A., "Electronic structure of pseudobinary semiconductor alloys Al<sub>x</sub>Ga<sub>1-x</sub>As, GaP<sub>x</sub>As<sub>1-x</sub>, and Ga<sub>x</sub>In<sub>1-x</sub>P" *Phys. Rev. B*, 23: 5360–5374 (1980).
- [3] Shimomura, A., Anan, T., Sugou, S., "Growth of AlPSb and GaPSb on InP by gas-source molecular beam epitaxy", *J. Cryst. Growth*, 162: 121-125 (1996).
- [4] Sahraoui, B., Dabos-Seignon, S., Migalska-Zalas, A., "Linear and nonlinear optical properties Zn<sub>1-x</sub>Mg<sub>x</sub>Se layers grown by MBE and LPD method" *Opto-Electronics Review*, 12: (4) 405-409 (2004).
- [5] Fredj, Debbichi, M., Said, M., "Influence of the composition fluctuation and the disorder on the bowing band gap in semiconductor materials", *Microelectronic J.*, 38: 860–870 (2007).
- [6] M. Robinson, P.D. Haynes, "Linear-scaling first-principles study of a quasicrystalline molecular material", *Chem. Phys. Lett.*, 476: 73-77 (2009).
- [7] Kohn, W., Sham, L.J., "Self-consistent equations including exchange and correlation effects", *Phys. Rev.*, 140: A1133–A1138 (1965).
- [8] Fischer, T H, Almlof, J., "General methods for geometry and wave function optimization", *J. Phys. Chem.*, 96: (24) 9768–9774 (1992).
- [9] Ceperley, D.M., Alder, B.J., "Ground state of the electron gas by a stochastic method", *Phys. Rev. Lett.*, 45: 566–569 (1980).
- [10] Perdew, J.P., Zunger, A., "Self-interaction correction to density-functional approximations for many-electron systems", *Phys. Rev. B*, 23: 5048–5079 (1981).
- [11] Troullier, N., Martins, "Efficient pseudopotentials for plane-wave calculations", *J. Phys. Rev. B*, 43: 1993–2006 (1993).
- [12] Vurgaftmana, I., Meyer, J.R., "Band parameters for III–V compound semiconductors and their alloys", *J. of Appl. Phys.*, 89: 5818- 5846 (2001).
- [13] Wang, S.Q., Yes, H.Q., "Plane-wave pseudopotentials study on mechanical and electronic properties for IV and III-V crystalline

- phases with zinc-blende structure”, *Phys. Rev. B*, 66: 2351111-235111 (2002).
- [14] Trägårdh, J., Persson, A.J., “Measurements of the band gap of wurtzite  $\text{InAs}_{1-x}\text{P}_x$  nanowires using photocurrent spectroscopy”, *J. of Appl. Phys.*, 101: 123701-123705 (2007).
- [15] Kim, T.J., Ghong, T.H., Kim, Y.D., “Dielectric functions of  $\text{In}_x\text{Ga}_{1-x}\text{As}$  alloys”, *Phys. Rev. B*, 68: 115323- 115339 (2003).
- [16] Serpone, N., Lawless, D., Khairutdinov, R., “Subnanosecond relaxation dynamics in  $\text{TiO}_2$  colloidal Sols (particle sizes  $R_p = 1.0\text{-}13.4$  nm). relevance to heterogeneous photocatalysis”, *J. Phys. Chem.*, 99: (45) 16655–16661 (1995).
- [17] Bachrach, R.Z., Haggi, B.W., “Magnetic hardening induced by ferromagnetic-antiferromagnetic”, *J. Appl. Phys.*, 89: 5103- 5106 (1971).